

This article was downloaded by: [Tomsk State University of Control Systems and Radio]

On: 21 February 2013, At: 10:47

Publisher: Taylor & Francis

Informa Ltd Registered in England and Wales Registered Number: 1072954
Registered office: Mortimer House, 37-41 Mortimer Street, London W1T 3JH, UK



Molecular Crystals and Liquid Crystals

Publication details, including instructions for authors and subscription information:

<http://www.tandfonline.com/loi/gmcl16>

Heat Capacity of N-p-n-Hexyloxybenzylidene-p'-n-butylaniline Between 11 and 393 K: Unusual Glassy Smectic Liquid Crystal

Hideki Yoshioka^{a b}, Michio Sorai^a & Hiroshi Suga^a

^a Chemical Thermodynamics Laboratory and Department of Chemistry, Faculty of Science, Osaka University, Toyonaka, Osaka, 560, Japan

^b Industrial Research Institute of Hyogo Prefecture, Yukihirocho, Sumaku, Kobe, 654, Japan

Version of record first published: 20 Apr 2011.

To cite this article: Hideki Yoshioka, Michio Sorai & Hiroshi Suga (1983): Heat Capacity of N-p-n-Hexyloxybenzylidene-p'-n-butylaniline Between 11 and 393 K: Unusual Glassy Smectic Liquid Crystal, *Molecular Crystals and Liquid Crystals*, 95:1-2, 11-30

To link to this article: <http://dx.doi.org/10.1080/00268948308072404>

PLEASE SCROLL DOWN FOR ARTICLE

Full terms and conditions of use: <http://www.tandfonline.com/page/terms-and-conditions>

This article may be used for research, teaching, and private study purposes. Any substantial or systematic reproduction, redistribution, reselling, loan,

sub-licensing, systematic supply, or distribution in any form to anyone is expressly forbidden.

The publisher does not give any warranty express or implied or make any representation that the contents will be complete or accurate or up to date. The accuracy of any instructions, formulae, and drug doses should be independently verified with primary sources. The publisher shall not be liable for any loss, actions, claims, proceedings, demand, or costs or damages whatsoever or howsoever caused arising directly or indirectly in connection with or arising out of the use of this material.

Heat Capacity of *N-p-n*-Hexyloxybenzylidene-*p'*-*n*- butylaniline between 11 and 393 K: Unusual Glassy Smectic Liquid Crystal[†]

HIDEKI YOSHIOKA,[‡] MICHIO SORAI, and HIROSHI SUGA

*Chemical Thermodynamics Laboratory and Department of Chemistry,
Faculty of Science, Osaka University, Toyonaka, Osaka 560, Japan*

(Received November 29, 1982)

Heat capacity measurements have been made on a 18 g sample of $C_6H_{13}O-C_6H_4-CH=N-C_6H_4-C_4H_9$ with an adiabatic-type calorimeter between 11 and 393 K. Purity of the specimen was estimated to be 99.93 mole % by a fractional fusion method. The transition temperature and the enthalpy and entropy of transition for crystal $\rightarrow S_G$, $S_G \rightarrow S_B$, $S_B \rightarrow S_A$, $S_A \rightarrow N$ and $N \rightarrow$ isotropic liquid were determined to be $T_c = 306.60$ K/ $\Delta H = 23.29$ kJ mol⁻¹/ $\Delta S = 75.98$ J K⁻¹ mol⁻¹, 331.56/0.84/2.53, 332.86/3.37/10.14, 343.24/3.20/9.37 and 350.92/1.89/5.37, respectively. A glassy S_G state was realized by rapid cooling. The heat capacity of the glassy state gave rise to two stepped anomalies due to the enthalpy relaxation around 200 K: a quite unusual phenomenon which has never been observed for other glassy liquid crystals, glassy liquids and glassy crystals. The molar enthalpy of the glassy S_G state at 0 K was by (9.27 ± 0.16) kJ mol⁻¹ higher than that of the crystalline state and the residual entropy of the glassy state was determined to be (7.51 ± 0.63) J K⁻¹ mol⁻¹.

1. INTRODUCTION

It has been known that, when a cooling rate is rapid enough, the lowest-temperature mesophase of many liquid crystals can be undercooled without

[†] Contribution No. 43 from Chemical Thermodynamics Laboratory.

[‡] Present address: Industrial Research Institute of Hyogo Prefecture, Yukihirocho, Sumaku, Kobe 654, Japan.

crystallization and finally transformed into a thermodynamically non-equilibrium glassy state *via* a glass transition region.

Of the glassy cholesteric,¹ nematic²⁻⁴ and smectic⁴ liquid crystals, the smectic glasses were found to exhibit a quite unusual glass transition phenomenon; it occurred over an extremely wide temperature interval of 30–60 K in contrast to a narrow range of 10–15 K encountered in the nematic and cholesteric glasses or ordinary isotropic liquid glasses. This fact seemed to suggest that in the glassy smectic state the relaxation time characterizing a rate at which the molecular modes frozen-in at the glass transition approach their equilibrium states cannot be described by a single value.⁴

In order to elucidate this problem we intended to measure the heat capacity of *N-p-n*-hexyloxybenzylidene-*p'*-*n*-butylaniline (abbreviated conventionally as 6O · 4; a typical compound among the glassy smectogens).⁴ This compound exhibits three smectic (S_G , S_B , and S_A) and one nematic (N) mesomorphic polymorphism.^{4,5} The present paper deals with heat capacity measurements from 11 to 393 K for all the stable phases as well as the glassy S_G phase. Since the analysis of the enthalpy relaxation has already been made in our previous report⁶ so the present paper will be concerned mainly with the thermodynamic relation of the glassy S_G state to the crystal and the polymorphic transitions.

2. EXPERIMENTAL

The methods of sample preparation and purification have been described previously.⁶ Purity of the specimen was determined to be 99.93 mole % based on a fractional fusion method.

The heat capacities were measured with an adiabatic-type calorimeter.⁷ The specimen of 18.0110 g (Δ 0.0533653 mol) was loaded in a calorimeter cell made of gold and platinum.⁸ A small amount of helium gas was used to aid the heat transfer inside the cell.

To estimate the contribution of intramolecular vibrations to the heat capacity, the infrared spectra in the range 4000–30 cm^{-1} were recorded for Nujol mulls with an Infrared Spectrophotometer Model DS-402G (Japan Spectroscopic Co., Ltd.) and a Far Infrared Spectrophotometer Model FIS-3 (Hitachi, Ltd.).

Optical textures of the crystal and mesophases were observed by a Polarizing Microscope Model BHA-751-P (Olympus) equipped with a heating stage (Union Optical Co., Ltd., Model CMS-2).

3. RESULTS

The results of the calorimetric measurements were evaluated in terms of C_p , the molar heat capacity at constant pressure, and are plotted in Figure 1. A listing of the experimental data is given in Table I. Consecutive runs during which the temperature increased monotonically are grouped into series.

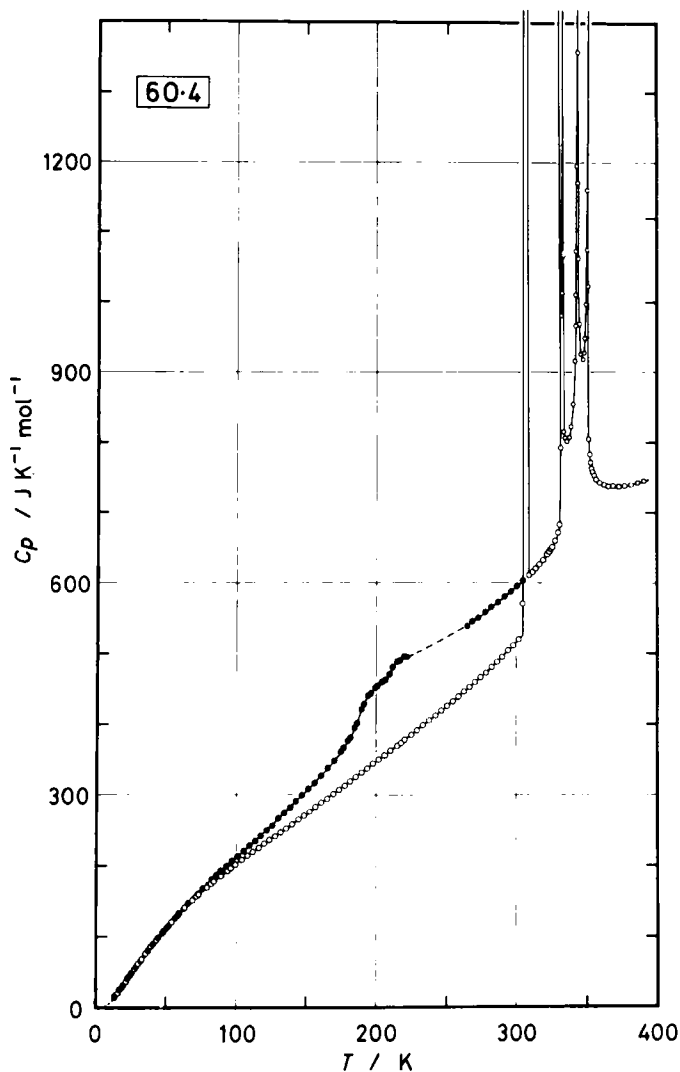


FIGURE 1 Molar heat capacity of $6O \cdot 4$. ○: The stable phases; the phase sequence being crystal, S_G , S_B , S_A , N and isotropic liquid. ●: The glassy and the undercooled S_G phases.

TABLE I
Molar heat capacity of *N-p-n*-hexyloxybenzylidene-*p'*-*n*-butylaniline

<i>T</i> /K	<i>C_p</i> /JK ⁻¹ mol ⁻¹	<i>T</i> /K	<i>C_p</i> /JK ⁻¹ mol ⁻¹	<i>T</i> /K	<i>C_p</i> /JK ⁻¹ mol ⁻¹
Δ <i>H</i> measurement		217.155	373.78	43.344	95.994
329.86 K → 338.63 K		219.952	378.15	45.348	100.40
Δ <i>H</i> measurement		224.339	385.02	47.524	105.21
338.63 K → 357.74 K		228.676	391.62	49.868	111.00
Once cooled to 78 K;		232.967	398.90	52.181	116.75
annealed at 303 K for 2 days;		237.214	405.34	Cooled again to 41.3 K	
cooled slowly to 70 K		241.870	412.40		
		246.022	419.47	Series 3 ^(b)	
Series 1 ^(a)		250.136	426.07		
73.437	159.36	254.211	432.54	42.346	94.618
76.678	164.93	258.247	439.44	44.410	98.346
79.348	169.52	262.245	446.09	46.527	103.13
81.939	173.89	266.204	452.99	48.674	107.58
82.427	174.83	270.125	459.79	50.784	113.11
84.670	177.95	274.010	466.57	53.172	118.88
84.753	178.54	278.089	473.38	55.677	124.67
87.030	182.25	282.093	481.19	58.271	130.40
89.261	185.86	286.058	488.35	60.956	135.82
91.448	189.16	289.982	495.71	63.666	141.10
93.540	192.92	293.864	504.49	66.105	145.75
96.122	196.44	297.714	510.98	68.450	150.29
99.704	201.88	301.454	519.91	71.036	155.10
103.893	207.99			74.655	161.57
107.966	214.02	Cooled slowly to 11.4 K		Annealed at 303 K for 2.5 days; cooled slowly to 41.5 K	
111.938	219.70			Series 4 ^(b)	
116.111	225.56	Series 2 ^(b)			
119.971	231.01	11.729	11.407	Series 5 ^(b)	
123.755	236.40	12.340	12.033		
127.807	241.97	13.005	13.778	42.595	94.194
131.628	247.63	13.712	15.735	44.646	98.798
135.715	253.38	14.598	18.057	46.746	103.64
140.061	259.49	15.630	20.927	49.030	108.40
144.333	265.61	16.529	23.190	Annealed at 47.8 K for 14 h	
148.534	271.50	17.453	25.645		
152.669	277.47	18.402	28.129	Series 6 ^(a)	
156.743	283.35	19.300	30.797		
160.759	289.23	20.289	33.534	44.711	98.993
165.028	295.44	21.607	37.460	46.428	102.34
169.171	301.75	23.166	41.939	48.053	106.67
173.258	307.72	24.636	46.180	48.976	109.48
177.292	313.67	25.950	49.817	Series 5 ^(b)	
181.278	319.12	27.419	54.147		
185.325	325.62	29.023	58.717	304.541	571.38
189.433	331.94	30.342	62.456	306.157	3984.9
193.493	337.75	31.870	66.638	306.500	54395.
197.507	344.25	33.619	71.406	306.538	122890.
201.675	350.11	35.476	76.475	306.557	176510.
205.609	356.08	37.330	81.237	306.571	234160.
209.829	362.63	39.303	86.318	306.581	317770.
214.327	369.44	41.334	91.070	306.590	315330.
				306.601	218370.
				307.264	1688.9

TABLE I (Continued)

T/K	$C_p/JK^{-1} \text{ mol}^{-1}$	T/K	$C_p/JK^{-1} \text{ mol}^{-1}$	T/K	$C_p/JK^{-1} \text{ mol}^{-1}$
309.109	611.09	351.479	804.63	28.971	58.454
311.480	615.89	352.075	783.57	30.311	62.320
313.962	621.46	352.678	770.82	31.587	65.743
316.554	626.79	353.286	763.26	32.573	68.481
319.130	632.74	354.050	757.81	33.902	72.088
321.697	640.87	355.277	752.89	35.626	76.746
323.163	645.09	356.855	747.41	37.578	81.840
324.243	648.97	359.177	742.99	39.474	86.585
325.191	651.85	362.282	739.87	41.373	91.082
327.204	660.59	365.392	737.85	43.306	95.832
329.199	672.08	368.963	738.25	45.288	100.27
330.518	683.17	372.987	737.98	47.302	104.86
331.145	792.54	377.250	738.45	48.793	108.51
331.561	2716.9	381.753	739.76	49.588	111.10
331.939	981.37	386.244	742.69	50.025	111.72
332.452	1013.5	390.634	745.29	50.270	112.58
332.745	9213.9	Undercooled S_G phase		50.515	112.71
332.802	19994.	down to 270.5 K		50.908	113.59
332.834	27070.	Series 7 ^(c)		52.101	116.45
332.859	31955.	272.842	550.85	54.073	120.83
333.116	1064.6	277.415	559.34	56.200	125.74
333.655	815.29	282.030	566.30	58.355	130.26
334.538	806.40	286.690	573.53	60.744	135.45
335.872	801.92	291.304	581.04	63.355	140.55
337.354	807.72	295.878	588.18	66.127	145.79
338.844	822.90	300.417	595.85	69.057	151.47
340.328	854.37	304.918	603.89	71.862	156.60
341.530	910.59	309.379	612.13	ΔH measurement	
342.129	966.46	Once cooled to 78 K;		301.48 K \rightarrow 313.23 K	
342.387	1011.4	annealed at 303 K for 2 days;		Undercooled S_G phase	
342.636	1073.7	cooled to 23 K; annealed at		down to 262.6 K	
342.871	1195.9	47.9 K for 24 h; cooled		Series 9 ^(c)	
343.080	1476.0	to 12 K.		264.471	539.45
343.208	5481.9	Series 8 ^(a)		268.249	545.78
343.244	40526.	12.415	12.252	Cooled rapidly from	
343.273	7230.2	13.251	14.414	342 K to 10.9 K	
343.399	1358.4	14.101	16.735	Series 10 ^(d)	
343.614	1171.7	14.965	19.038	11.188	10.636
343.972	1062.8	15.843	21.475	11.933	12.589
344.869	969.67	16.749	23.757	12.856	14.822
346.218	926.07	17.681	26.313	13.841	17.583
347.341	918.08	18.622	28.837	14.832	20.192
348.157	927.51	19.574	31.454	15.845	22.887
348.964	949.24	20.536	34.191	16.869	25.434
349.752	996.70	21.505	37.187	17.999	28.265
350.322	1075.4	22.579	40.181	19.190	31.495
350.619	1160.2	23.737	43.520	20.360	34.639
350.826	1580.0	24.950	46.934	21.566	37.974
350.920	103130.	26.214	50.642	22.851	41.628
350.927	35414.	27.563	54.453		
351.058	1022.8				

TABLE I (Continued)

<i>T</i> /K	<i>C_p</i> /JK ⁻¹ mol ⁻¹	<i>T</i> /K	<i>C_p</i> /JK ⁻¹ mol ⁻¹	<i>T</i> /K	<i>C_p</i> /JK ⁻¹ mol ⁻¹
24.210	45.365	179.485	376.42		
25.606	49.109	184.332	395.49		
27.033	53.120	189.176	421.33		
28.501	57.214	194.007	439.98		
30.007	61.429	198.894	451.13		
31.799	66.249	203.922	459.57		
33.758	71.541	209.095	470.44		
35.536	76.288	214.225	488.02		
37.237	80.741	219.322	495.78		
38.958	85.175				
40.726	89.415	Measurement of the enthalpy of crystallization			
42.575	94.042	Cooled rapidly from 342 K to			
44.522	98.645	90 K			
46.506	103.19				
48.451	108.03	Series 11 ^(d)			
50.225	112.15	176.459	367.10		
51.752	115.61	181.281	381.68		
53.770	120.22	186.155	401.84		
56.396	126.45	191.019	428.95		
59.421	133.34	195.879	443.69		
62.623	140.17	200.788	454.44		
65.919	147.15	205.849	462.34		
69.339	154.39	211.101	480.72		
72.806	161.43	216.398	490.02		
76.197	168.15	221.821	494.96		
79.528	174.73				
82.826	181.00				
86.123	186.92				
89.458	193.06				
93.048	199.47				
96.948	206.36				
100.959	213.41				
105.184	221.31				
109.262	228.65				
113.358	235.64				
117.476	242.75				
121.629	250.19				
125.802	258.46				
129.986	267.25				
134.171	275.02				
138.386	282.83				
142.644	291.36				
146.982	299.94				
151.412	308.59				
155.918	317.96				
160.504	327.68				
165.163	338.34				
169.891	349.01				
174.669	361.35				

(a) stable phases; (b) not completely annealed crystalline phase; (c) undercooled S_G phase;
(d) glassy S_G phase.

Prior to heat capacity measurements of the crystalline phase the specimen was once cooled to 78 K and annealed for 2 days at 303 K, a temperature just below the melting point. This procedure promoted nucleation and its growth of the stable crystal. After cooling the specimen slowly to 70 K the measurements of series 1 were made up to 303 K. The calorimeter was then cooled slowly to 11.4 K and series 2 was started. However, since slight spontaneous warming was observed in the region between 45 and 50 K, the measurements were terminated at 54 K. Even after further annealing under various conditions, spontaneous warming still occurred in series 3–5 as it had during series 2. This phenomenon, however, did not appear in the measurements of series 8 subject to the eventual heat treatments cited in Table I. A possible origin responsible for the spontaneous warming may be a kind of relaxation phenomenon of molecular conformation or configuration in a crystalline state.^{9,10} In any event this effect is negligibly small in the present system because we cannot distinguish the heat capacities of the well-annealed specimen from those of the quenched one within the present experimental errors.

Series 6 covers the temperature region including all the mesomorphic transitions as well as the fusion of crystal. Purity of the specimen was determined to be 99.93 mol % by a fractional fusion method. The melting point of the present sample was 306.60 K while the triple point of pure material was estimated to be 306.62 K. The S_G phase was transformed into S_B at 331.56 K, immediately followed by a transition to S_A at 332.86 K; the temperature interval of the S_B phase being as narrow as 1.30 K. The transition from S_A to the nematic state took place at 343.24 K and finally the nematic phase was transformed into the isotropic liquid at 350.92 K (the clearing point).

The heat capacities of the glassy S_G state were measured in series 10 and 11 for the specimen cooled from 342 K to 10.9 and 90 K at an average rate of 7.2 and 6.7 K min⁻¹, respectively. Although, at the starting temperature of cooling, the specimen was in the S_A state we confirmed that the obtained glassy state was undoubtedly S_G for the reasons described previously.⁶ As shown in Figure 1 by solid circles, the heat capacity of the glassy S_G state progressively deviated from that of the crystal above 60 K and its magnitude became larger with increasing temperature. It finally gave rise to two stepped anomalies around 200 K and then the glassy state was transformed into the undercooled S_G state.

When temperature of the specimen reached about 225 K, a large evolution of heat was observed due to an irreversible transition from the undercooled S_G to the crystalline phase. On account of this disturbance, heat capacity measurements of the undercooled S_G state could not be continued in these series of experiments. However, the temperature rise due to

the crystallization could be followed while keeping adiabatic conditions in the calorimeter. From this experiment, the heat of crystallization was accurately determined and thus the molar enthalpy of the glassy state could be related with the crystal enthalpy.

On the other hand, the C_p in a high-temperature region of the undercooled S_G state could be measured in series 7 and 9 for the specimen cooled from the stable S_G state down to 270.5 and 262.6 K, respectively. Since further cooling brought about spontaneous crystallization, the C_p measurements below 260 K were impossible. Therefore, the heat capacities of the undercooled S_G state in the range from 225 to 260 K were estimated in reference to the enthalpy diagram so that the area under the assumed C_p curve in this temperature interval may coincide with the enthalpy difference between these two temperatures. The heat capacities thus estimated are given by the following equation,

$$C_p(\text{undercooled } S_G)/\text{J K}^{-1} \text{ mol}^{-1} = 3.086 \times 10^{-3}T^2 - 0.461T + 447.3 \quad (225 \leq T/\text{K} \leq 260), \quad (1)$$

and are illustrated in Figure 1 by a broken line.

The thermodynamic functions of $6\text{O} \cdot 4$ were calculated from the heat capacity data and the calorimetric enthalpy measurements across the respective phase transitions. In order to estimate the heat capacities of the crystalline and the glassy S_G states below 11 K, an effective frequency spectrum method¹¹ was adopted. To this end, infrared absorption data of 32 modes (102 degrees of freedom) between 3040 and 545 cm^{-1} were used. The 'best' frequency spectrum reproduced 58 C_p data for the crystal in the range 12.4–108.0 K within $\pm 0.23 \text{ J K}^{-1} \text{ mol}^{-1}$ while for the glassy S_G state 50 C_p data between 11.2 and 125.8 K were fitted within $\pm 0.47 \text{ J K}^{-1} \text{ mol}^{-1}$. Table II contains a listing of values for the heat capacity, C_p° , the entropy, S° , the enthalpy function, $(H^\circ - H_0^\circ)/T$ and the Gibbs energy function, $-(G^\circ - H_0^\circ)/T$, at selected temperatures. Corresponding values for the glassy and undercooled S_G states are listed in Table III, in which a standard state of the enthalpy at 0 K has been taken as that of the crystal, $H_0^\circ(\text{crystalline})$.

The mesophases were distinguishable from one another under a polarizing microscope equipped with a heating stage. Figures 2(a)–(d) show optical textures of the four mesophases photographed on cooling; (a) N : schlieren texture with surface inversion lines, (b) S_A : bâtonnets, (c) S_B : fan-shaped texture and (d) S_G : paramorphic fan-shaped texture with concentric arcs. Figure 2(e) corresponds to a texture of the crystalline state formed by cooling with cold N_2 gas. On heating, the texture of the S_A phase changed from bâtonnets (Figure 2(b)) to fan-shaped texture with additional

TABLE II

Standard thermodynamic functions for the stable phases of *N-p-n*-hexyloxybenzylidene-*p'*-*n*-butylaniline in $\text{JK}^{-1} \text{mol}^{-1}$ (relative molecular mass 337.504)

T/K	C_p°	S°	$(H^\circ - H_0^\circ)/T$	$-(G^\circ - H_0^\circ)/T$
5	(1.09)	(0.373)	(0.279)	(0.094)
10	(7.28)	(2.669)	(1.968)	(0.701)
20	32.67	15.051	10.653	4.397
30	61.42	33.765	22.819	10.946
40	87.83	55.136	35.854	19.283
50	111.69	77.275	48.600	28.675
60	133.84	99.619	61.004	38.615
70	153.20	121.73	72.811	48.916
80	170.62	143.33	83.960	59.371
90	186.97	164.47	94.581	69.885
100	202.31	184.97	104.63	80.338
120	231.05	224.42	123.32	101.10
140	259.40	262.17	140.74	121.42
160	288.12	298.67	157.35	141.31
180	317.37	334.31	173.52	160.79
200	347.66	369.33	189.43	179.90
220	379.06	403.89	205.20	198.68
240	409.56	438.14	220.91	217.23
260	442.36	472.21	236.68	235.53
280	477.11	506.51	252.86	253.66
298.15	512.02	537.57	267.58	269.98
300	516.44	540.75	269.10	271.65
310	612.89	634.85	353.39	281.46
320	635.50	654.64	361.83	292.81
340	847.42	709.29	393.73	315.56
360	742.16	765.20	426.07	339.13
380	739.25	805.14	442.52	362.62
390	744.92	824.41	450.20	374.21

discontinuities (Figure 2(f)). Here, the assignment of textures has been made according to a literature.¹²

4. ENTHALPY AND ENTROPY OF PHASE TRANSITION

As the mesomorphic transition takes place successively before the heat capacity anomaly of the preceding transition has not terminated, estimation of the enthalpy and entropy of the respective phase transitions involves more or less ambiguity. We determined base lines of heat capacity, C_p (normal), which separate the excess part due to the phase transitions, ΔC_p , from the observed values, on the following assumptions;

- (i) $C_{p(\text{normal})}$ for all the phases be approximated by straight lines,

TABLE III

Thermodynamic functions for the glassy and undercooled S_G phases of
N-p-n-hexyloxybenzylidene-*p'*-*n*-butylaniline in $\text{JK}^{-1} \text{mol}^{-1}$; H_0° means the
 enthalpy of the stable crystalline phase at 0 K

T/K	C_p°	S°	$(H^\circ - H_0^\circ)/T$	$-(G^\circ - H_0^\circ)/T$
$S_0^\circ = (7.51 \pm 0.63) \text{ JK}^{-1} \text{mol}^{-1}$ $H_0^\circ (\text{glassy } S_G) - H_0^\circ (\text{crystalline}) = (9.27 \pm 0.16) \text{ kJ mol}^{-1}$				
10	(8.47)	(11.214)	(929.15)	(-917.94)
20	33.67	24.513	474.79	-450.27
30	61.41	43.398	332.38	-288.98
40	87.67	64.722	267.96	-203.24
50	111.62	86.876	234.32	-147.44
60	134.58	109.26	215.82	-106.56
70	155.73	131.60	205.74	-74.14
80	175.62	153.71	200.74	-47.03
90	194.02	175.47	198.98	-23.51
100	211.72	196.83	199.38	-2.55
120	247.27	238.61	204.42	34.19
140	286.06	279.39	213.08	66.31
160	326.61	319.92	224.45	95.47
180	378.44	360.77	238.10	122.67
200	452.85	404.67	256.02	148.65
220	493.30	449.41	275.47	173.94
240 ^(a)	511.96	493.17	294.41	198.77
260 ^(a)	534.80	535.02	311.99	223.03
280	563.23	575.61	328.85	246.77
300	595.14	615.04	345.05	269.99
310	612.89	634.85	353.39	281.46

(a) The values at these temperatures are estimated based on the interpolation curve (Eq. (1)).

$$C_p (\text{normal}) = AT + B. \quad (2)$$

(ii) ΔC_p be described by

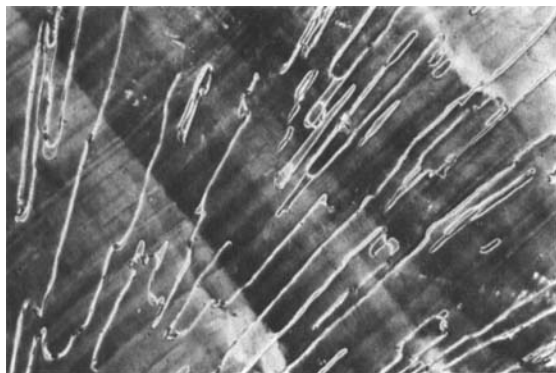
$$\ln \Delta C_p = C - D \ln \epsilon \quad (\epsilon \equiv |T - T_c|/T_c), \quad (3)$$

as if each phase transition could be treated as the so-called critical phenomenon.

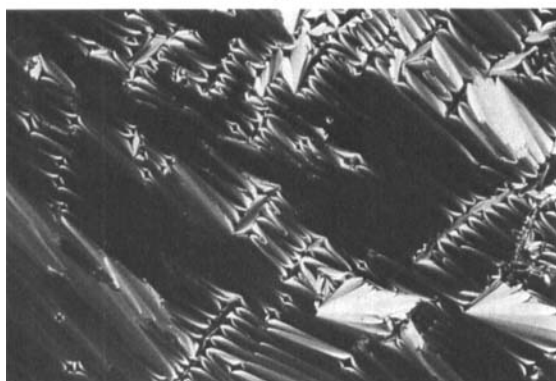
(iii) The slopes of $C_p(\text{normal})$ for S_A and N phases be determined on reference to those for S_G and isotropic liquid phases, respectively.

(iv) ΔC_p does not exert its effect beyond the adjacent transition points.

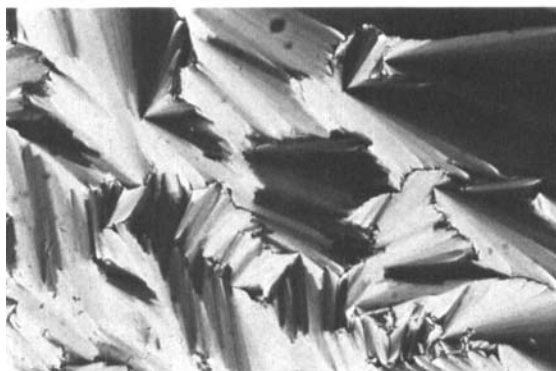
(v) As the temperature interval of S_B phase is as narrow as 1.30 K, C_p (normal) of this phase be approximated by that of S_G . The $C_p(\text{normal})$ thus estimated are given by the following equations in the unit of $\text{J K}^{-1} \text{mol}^{-1}$,



(a)



(b)

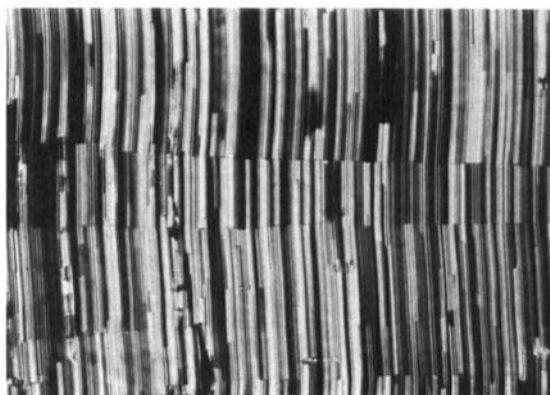


(c)

FIGURE 2 Optical textures of the mesomorphic and crystalline states of $6O \cdot 4$; (a) N, (b) S_A , (c) S_B , (d) S_G on cooling, (e) crystal and (f) S_A on heating. Magnification is $100\times$ for



(d)



(e)



(f)

FIGURE 2 (continued)

$$\begin{array}{ll}
 \text{(A) } C_p(\text{normal, K}) & = 1.9929T - 80.86, \\
 \text{(B) } C_p(\text{normal, } S_G \text{ and } S_B) & = 1.7265T + 77.60, \\
 \text{(C) } C_p(\text{normal, } S_A) & = 1.7265T + 107.60, \\
 \text{(D) } C_p(\text{normal, N}) & = 0.52481T + 640.04, \\
 \text{(E) } C_p(\text{normal, IL}) & = 0.52481T + 540.04,
 \end{array} \quad (4)$$

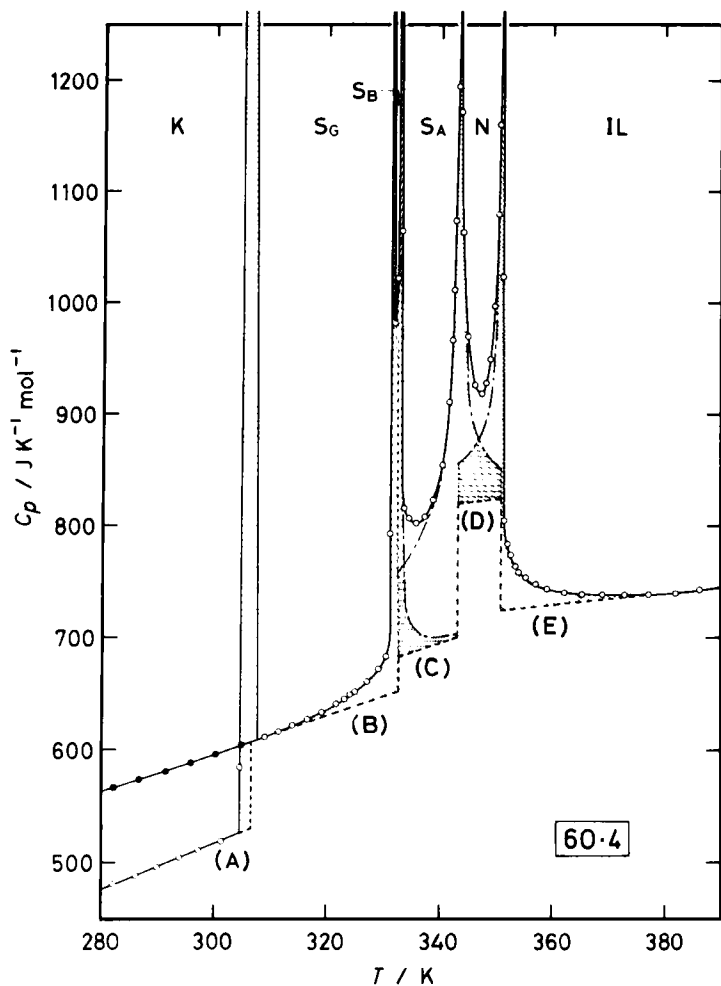


FIGURE 3 Separation of the excess heat capacities due to phase transitions from the experimental values. Broken lines labeled (A), (B), (C), (D) and (E) are given by Eq. (4). Excess heat capacities of the respective phase transitions are shown by dot-dash lines. The hatched areas correspond to the enthalpies of respective phase transitions. K, S, N and IL are abbreviations of crystal, smectic, nematic and isotropic liquid phases, respectively.

and illustrated in Figure 3 by broken lines. Values of the constants C and D used in Eq. (3) are listed in Table IV and the ΔC_p of each phase transition are shown in Figure 3 by dot-dash lines.

The enthalpy and entropy of transition were determined by integrating the excess heat capacity with respect to T and $\ln T$, respectively. For these calculations, the results of the calorimetric enthalpy measurements across the respective phase transitions were also taken into account. Table V contains a listing of thermodynamic values concerning the phase transitions. The temperature dependence of the entropy acquisition due to the phase transitions is represented in Figure 4. The individual transition entropy can be compared with available data for p' -substituted p -*n*-hexyloxybenzylideneanilines. The $\Delta S(N \rightarrow IL)$ of $5.37 \text{ J K}^{-1} \text{ mol}^{-1}$ is slightly high compared with $3.2(\text{HBAB})$,⁸ $3.5(\text{HBAF})$ ¹³ and $3.9 \text{ J K}^{-1} \text{ mol}^{-1}(\text{HBT})$.¹⁴ This may be accounted for in terms of additional degrees of freedom in the present molecule. In contrast to this, the $\Delta S(S_A \rightarrow N)$ of $9.37 \text{ J K}^{-1} \text{ mol}^{-1}$ is nearly identical with $10.2 \text{ J K}^{-1} \text{ mol}^{-1}(\text{HBAF})$,¹³ and the $\Delta S(S_B \rightarrow S_A)$ of $10.14 \text{ J K}^{-1} \text{ mol}^{-1}$ is compatible with $9.2(\text{HBAF})$ ¹³ and $9.3 \text{ J K}^{-1} \text{ mol}^{-1}(\text{HBAC})$.¹⁵ Although there exist no available calorimetric data for $\Delta S(S_G \rightarrow S_B)$ to be compared, the

TABLE IV

Values of the constants C and D used in Eq. (3):
 $\ln(\Delta C_p/\text{JK}^{-1} \text{ mol}^{-1}) = C - D \ln \epsilon$ ($\epsilon \equiv |T - T_c|/T_c$)

Applied phase	T_c/K	C	D
S_G and S_B	332.86	-0.52853	0.77486
S_A	332.86	-2.3986	1.1068
S_A	343.24	2.4318	0.55241
N	343.24	-0.19610	0.91399
N	350.92	0.92439	0.69049
IL	350.92	0.42436	0.64107

TABLE V

Enthalpy and entropy of phase transitions in
N-*p*-*n*-hexyloxybenzylidene-*p'*-*n*-butylaniline

Transition	T_c/K	$\Delta H/\text{kJ mol}^{-1}$	$\Delta S/\text{JK}^{-1} \text{ mol}^{-1}$
crystal \rightarrow smectic-G	306.60	23.29	75.98
smectic-G \rightarrow smectic-B	331.56	0.84	2.53
smectic-B \rightarrow smectic-A	332.86	3.37	10.14
smectic-A \rightarrow nematic	343.24	3.20	9.37
nematic \rightarrow isotropic liquid	350.92	1.89	5.37
			total 103.4

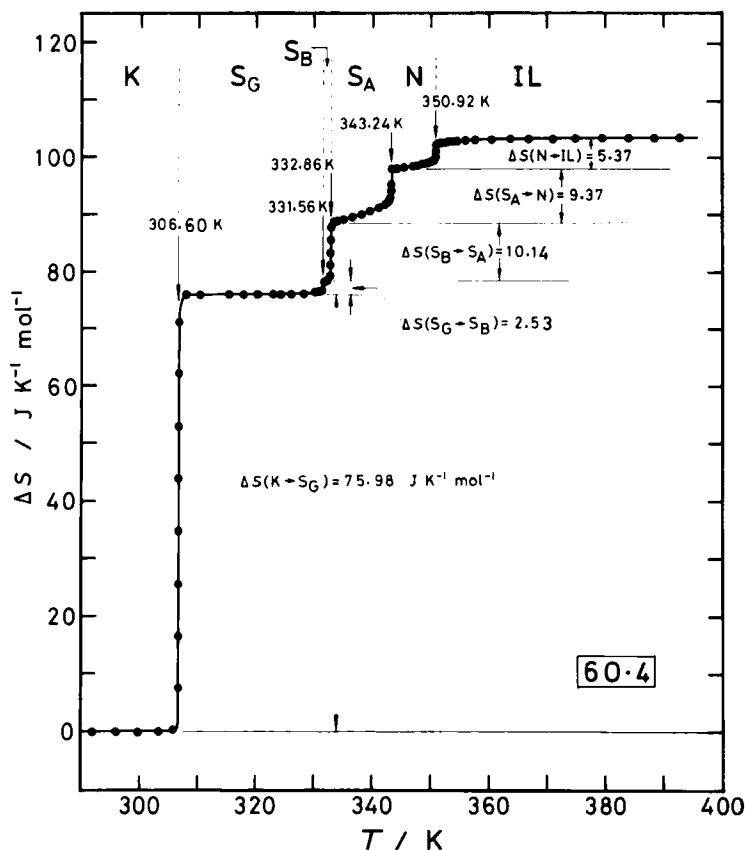


FIGURE 4 Temperature dependence of the entropy acquisition due to the melting and mesomorphic transitions for 6O · 4.

small value of the present result ($2.53 \text{ J K}^{-1} \text{ mol}^{-1}$) affords a clear evidence that the structures of S_G and S_B phases resemble each other from a thermodynamic viewpoint.

On the other hand, if we compare the cumulative transition entropy with that of HBT (alternatively abbreviated as 6O · 1; a compound bearing the closest resemblance to the present 6O · 4 among those quoted above), we perceive an interesting fact that, despite of three excess methylene groups in the present molecule, the cumulative entropy of $103.4 \text{ J K}^{-1} \text{ mol}^{-1}$ is only by $9.6 \text{ J K}^{-1} \text{ mol}^{-1}$ larger than $93.79 \text{ J K}^{-1} \text{ mol}^{-1}$ for HBT.¹⁴ As the entropy increment per methylene group¹⁶ is about $(10.31 \pm 0.53) \text{ J K}^{-1} \text{ mol}^{-1}$, an expected value of the cumulative entropy for the present compound amounts to *ca.* $125 \text{ J K}^{-1} \text{ mol}^{-1}$ as far as it is estimated on the

basis of HBT. However, if we compare the heat capacities of the two substances in the crystalline states, this puzzle can be easily solved. Let's compare the values at 200 K as an example. Since the values of $6O \cdot 4$ and $6O \cdot 1^{14}$ are 347.66 and $286.31 \text{ J K}^{-1} \text{ mol}^{-1}$, respectively, so the heat capacity difference at 200 K is $61.35 \text{ J K}^{-1} \text{ mol}^{-1}$. This value considerably exceeds $44.1 \text{ J K}^{-1} \text{ mol}^{-1}$; the value¹⁷ expected for the heat capacity increment per three methylene groups in crystalline state. In other words, these facts suggest that a great extent of the conformational melting of the butyl-constituent in the present compound has already proceeded in the crystalline state.

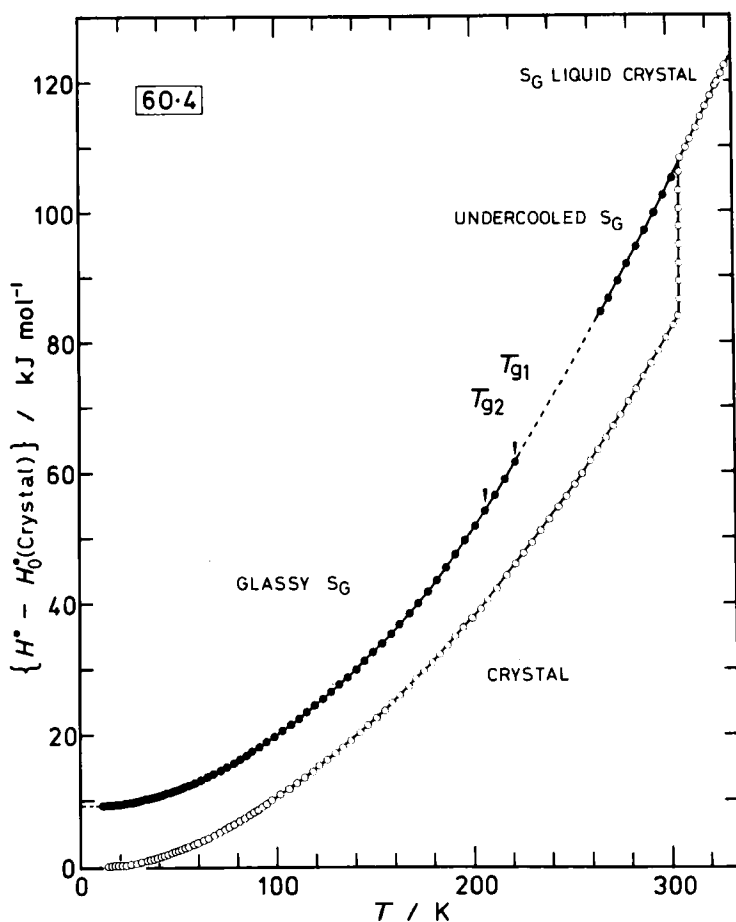


FIGURE 5 The enthalpy diagram correlating various phases of $6O \cdot 4$.

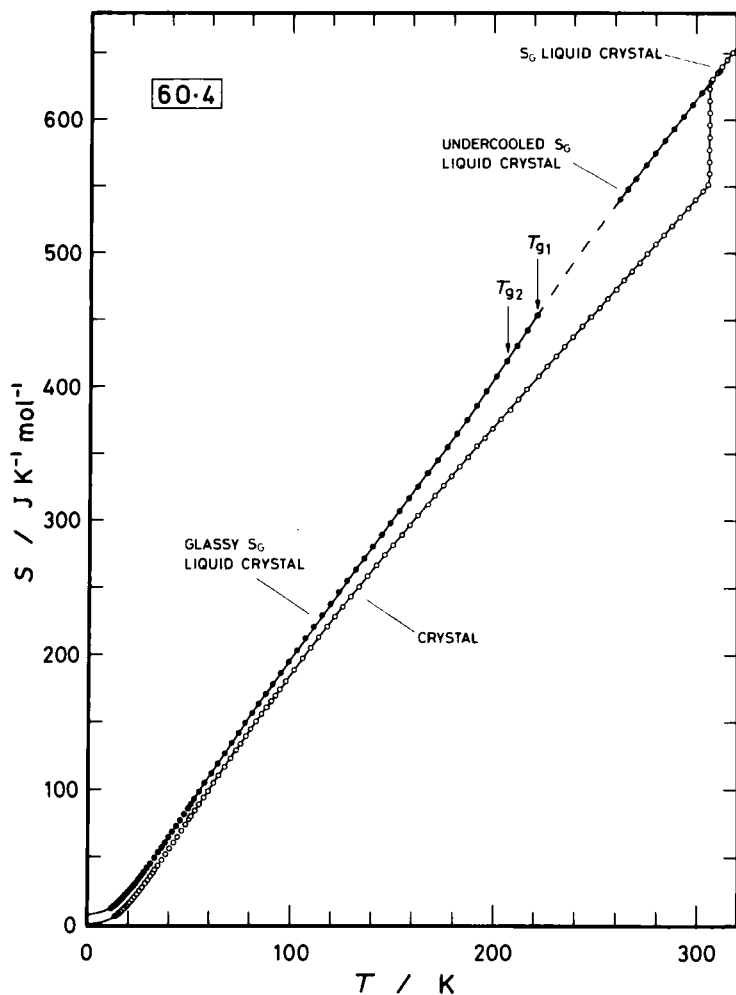


FIGURE 6 The entropy diagram correlating various phases of 6O·4.

5. GLASSY SMECTIC STATE

Calorimetry provides decisive evidences to identify a glassy state; they involve (i) the residual entropy at 0 K, (ii) existence of glass transition 'point', T_g , or region and (iii) enthalpy relaxation phenomenon around T_g .

As mentioned in Section 3, the molar enthalpy of the glassy S_G state could be correlated with that of the crystalline state by measuring the enthalpy of crystallization around 225 K while keeping an adiabatic condi-

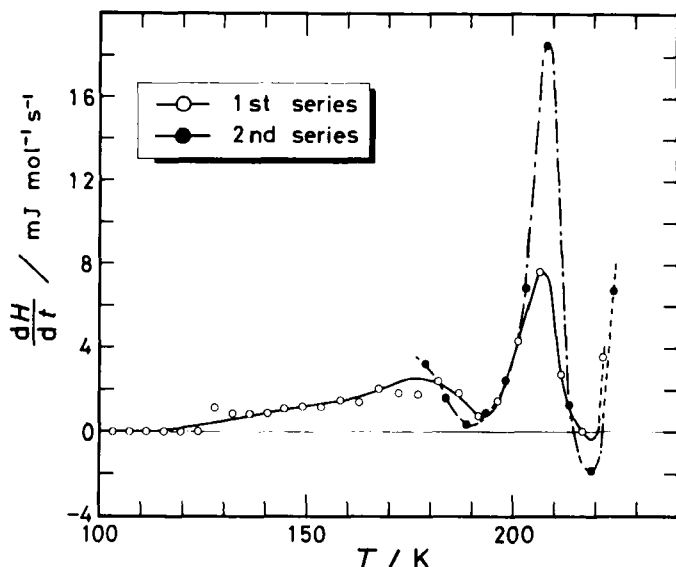


FIGURE 7 Temperature dependence of the rate of enthalpy relaxation, dH/dt , in the glass transition region. First and second series of experiments correspond to the measurements of series 10 and 11 in Table I, respectively. Broken lines drawn above 220 K indicate spontaneous warming due to crystallization.

tion in the calorimeter. The enthalpy diagram relating various phases is shown in Figure 5. The enthalpy difference between the glassy S_G and crystalline states at 0 K was determined to be (9.27 ± 0.16) kJ mol $^{-1}$. Similar diagram concerning the entropy is given in Figure 6. By assuming that the crystalline state obeys the third law of thermodynamics the residual entropy of the glassy S_G state at 0 K was estimated to be (7.51 ± 0.63) JK $^{-1}$ mol $^{-1}$. This value is much smaller than 12.69 JK $^{-1}$ mol $^{-1}$ for the glassy nematic state of OHMBBA.³ This fact reflects the situation that molecular order is much higher in a smectic-G state than in a nematic one.

The most remarkable feature inherent in the present smectic glass manifests itself in the glass transition phenomenon. As shown in Figure 7, the enthalpy relaxation was detected from as low as 120 K, and furthermore of much interest is the fact that the temperature dependence of the enthalpy relaxation rate, dH/dt , evidently shows a pair of glass transitions. These facts just correspond to the widely spread excess heat capacity and the existence of two stepped heat capacity anomalies of the glassy S_G state, respectively (see Figure 8). The multi-glass-transition reflects the fact that there exist multi-relaxation processes in the present smectic glass.

Since this kind of double glass transition phenomenon has never been observed for nematic and cholesteric glasses, ordinary isotropic liquid

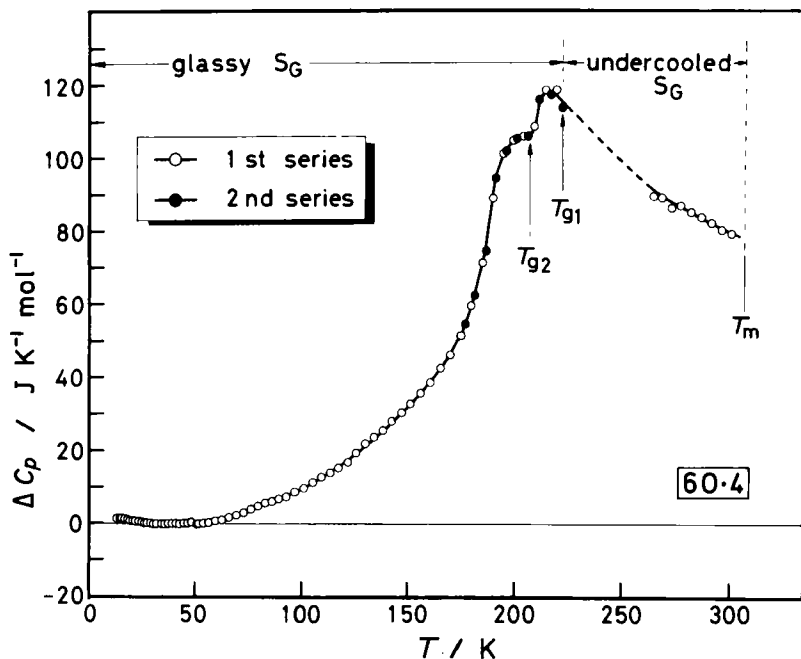


FIGURE 8 Excess heat capacities of the glassy and undercooled S_G states beyond the crystalline state. First and second series of experiments correspond to the measurements of series 10 and 11 in Table I, respectively. The temperatures at which the relaxation times become 1 ks are indicated by T_{g1} and T_{g2} .

glasses and glassy crystals,^{9,10} we thought that this phenomenon might be caused by the intrinsic nature of a smectic state. The most characteristic feature of smectic phases differentiated from other liquid crystalline phases is that molecules are arranged in layer structures. Therefore, at least one of the double glass transitions should have its origin in a freezing of molecular modes characteristic of a layer structure. Plausible molecular modes proper to a layer structure are the undulation mode of a layer^{18,19} or anisotropic translational self-diffusions parallel and perpendicular to a smectic layer.²⁰ As we have fully discussed these possibilities previously,⁶ we shall conclude this paper by remarking that it is urgent to examine whether a similar double glass transition phenomenon will be observed for other smectic states such as S_A , S_B , S_C , *etc.* and even for S_G states of other compounds.

Acknowledgment

The authors acknowledge Itoh Science Foundation for supplying them a polarization microscope equipped with a heating stage.

References

1. K. Tsuji, M. Sorai, and S. Seki, *Bull. Chem. Soc. Japan*, **44**, 1452 (1971).
2. M. Sorai and S. Seki, *Bull. Chem. Soc. Japan*, **44**, 2887 (1971).
3. M. Sorai and S. Seki, *Mol. Cryst. Liq. Cryst.*, **23**, 299 (1973).
4. M. Sorai, T. Nakamura, and S. Seki, *Pramana, Suppl. I*, 503 (1975).
5. J. B. Flannery, Jr. and W. Haas, *J. Phys. Chem.*, **74**, 3611 (1970).
6. M. Sorai, H. Yoshioka, and H. Suga, *Liquid Crystals and Ordered Fluids*, ed. A. C. Griffin and J. F. Johnson, Vol. 4 (1983), Plenum Press.
7. M. Yoshikawa, M. Sorai, H. Suga, and S. Seki, *J. Phys. Chem. Solids*, **44**, — (1983).
8. K. Tsuji, M. Sorai, H. Suga, and S. Seki, *Mol. Cryst. Liq. Cryst.*, **55**, 71 (1979).
9. H. Suga and S. Seki, *J. Non-Cryst. Solids*, **16**, 171 (1974).
10. H. Suga and S. Seki, *Faraday Discussions*, **69**, 221 (1980).
11. M. Sorai and S. Seki, *J. Phys. Soc. Japan*, **32**, 382 (1972).
12. D. Demus and L. Richter, *Textures of Liquid Crystals*, Verlag Chemie, Weinheim (1978).
13. K. Tsuji, M. Sorai, H. Suga, and S. Seki, *Mol. Cryst. Liq. Cryst.*, **87**, 305 (1982).
14. K. Tsuji, M. Sorai, H. Suga, and S. Seki, *Mol. Cryst. Liq. Cryst.*, **90**, 97 (1982).
15. K. Tsuji, M. Sorai, H. Suga, and S. Seki, *Mol. Cryst. Liq. Cryst.*, **87**, 293 (1982).
16. M. Sorai, K. Tsuji, H. Suga, and S. Seki, *Mol. Cryst. Liq. Cryst.*, **59**, 33 (1980).
17. H. Finke, M. E. Gross, G. Waddington, and H. H. Huffman, *J. Am. Chem. Soc.*, **76**, 333 (1954).
18. P. G. de Gennes, *J. Phys. (Paris)*, **30**, C4–65 (1969).
19. R. Ribotta, D. Salin, and G. Durand, *Phys. Rev. Lett.*, **32**, 6 (1974).
20. W. J. LaPrice and D. L. Uhrich, *J. Chem. Phys.*, **72**, 678 (1980).